The hydration of the OH radical: Microsolvation modeling and statistical mechanics simulation

P. Cabral do Couto, R. C. Guedes, and B. J. Costa Cabral[a)]
Departamento de Química e Bioquímica, Faculdade de Ciências, Universidade de Lisboa, 1749-016 Lisboa, Portugal and Grupo de Física Matemática da Universidade de Lisboa, Av. Professor Gama Pinto 2, 1649-003 Lisboa, Portugal

J. A. Martinho Simões
Departamento de Química e Bioquímica, Faculdade de Ciências, Universidade de Lisboa, 1749-016 Lisboa, Portugal

(Received 12 June 2003; accepted 15 July 2003)

The hydration of the hydroxyl OH radical has been investigated by microsolvation modeling and statistical mechanics Monte Carlo simulations. The microsolvation approach was based on density functional theory (DFT) calculations for $OH-(H_2O)_{1-6}$ and $(H_2O)_{1-7}$ clusters. The results from microsolvation indicate that the binding enthalpies of the OH radical and water molecule to small water clusters are similar. Monte Carlo simulations predict that the hydration enthalpy of the OH radical, $\Delta_{hyd}H(OH,g)$, is $-39.1\ kJ\,mol^{-1}$. From this value we have estimated that the band gap of liquid water is 6.88 eV, which is in excellent agreement with the result of Coe *et al.* [J. Chem. Phys. **107**, 6023 (1997)]. We have compared the structure of the hydrated OH solution with the structure of pure liquid water. The structural differences between the two systems reflect the strong role played by the OH radical as a proton donor in water. From sequential Monte Carlo/DFT calculations the dipole moment of the OH radical in liquid water is 2.2 ± 0.1 D, which is ~33% above the experimental gas phase value (1.66 D). © *2003 American Institute of Physics.*
[DOI: 10.1063/1.1605939]

I. INTRODUCTION

The interaction of the hydroxyl radical with biological molecules, including amino acids, peptides, and proteins, is of great interest due to the deleterious effects of the radical on biological systems.[1–4] For example, high concentrations of the hydroxyl (OH) radical in the cell cytoplasm have been associated with Parkinson's disease.[5] The OH radical is also important in the chemistry of earth's atmosphere, where its role in hydrogen abstraction reactions determines the atmospheric lifetime of many hydrofluorocarbons.[6–8] Most of the reactions involving the OH radical occur in aqueous environment or in small water aggregates that can act as catalysts in some atmospheric reactions.[9] The study of OH radical hydration is therefore very important because the oxidation mechanisms of organic molecules by aqueous OH will depend strongly on the structural and energetic properties of the hydrated radical.[10,11] Another relevant issue concerns the electronic properties of liquid water, where the adiabatic band gap of the liquid, which can be determined over thermochemical cycles involving the OH^- defect state in water, depends on the OH radical hydration energy.[12]

Several works have been carried out to analyze the interactions of the OH radical with the water molecule[13–16] and the microsolvation of the radical in water clusters.[12,17] In the present paper we report a theoretical study of the hydration of the OH radical. To carry out this study two approaches have been adopted: microsolvation modeling and Monte Carlo statistical mechanics simulations. Initially, we have analyzed the microsolvation of the OH radical in water (W) by carrying out density functional theory (DFT) calculations for $OH-W_N$ clusters ($N=1-6$), where N is the number of water molecules. From these calculations, several properties, including the structure, energetics, vibrational spectrum, and charge distribution have been determined and compared with the properties of water clusters W_{N+1} ($N=1-6$). Monte Carlo simulations were then carried out to analyze the structure of the hydrated hydroxyl solution and to predict the OH radical enthalpy of hydration, $\Delta_{hyd}H(OH,g)$. Finally, sequential Monte Carlo/DFT calculations over uncorrelated configurations[18,19] of the solution have been performed to investigate the electronic polarization of the hydroxyl radical in liquid water.

II. COMPUTATIONAL DETAILS

To analyze the structure, vibrational spectrum, and energetics of $OH-W_N$ ($N=1-6$) clusters, where $W=H_2O$ and N is the number of water molecules, we have carried out density functional theory calculations with the Adamo and Barone[20–22] Becke style one-parameter hybrid functional, using a modified Perdew–Wang exchange[22] and PW91 correlation[23] (MPW1PW91). The geometries of $OH-W_N$ and W_{N+1} clusters ($N=1-6$) have been fully optimized with Dunning's correlation consistent polarized valence double

a)Author to whom all correspondence should be addressed. Electronic mail: ben@adonis.cii.fc.ul.pt

 © 2003 American Institute of Physics

Downloaded 27 May 2007 to 194.117.6.7. Redistribution subject to AIP license or copyright, see http://jcp.aip.org/jcp/copyright.jsp

zeta basis set augmented with diffuse functions (aug-cc-pVDZ).[24] Single-point energy calculations with the aug-cc-pVTZ and aug-cc-pVQZ basis sets[25] are also reported.

The energetics of the OH–W_N clusters can be discussed in terms of the formation and binding energies. The formation energy $\Delta E_{e,N}$ is defined as

$$\Delta E_{e,N} = E[\mathrm{OH}-\mathrm{W}_N] - E[\mathrm{OH}] - NE[\mathrm{W}_1], \tag{1}$$

where $E[\mathrm{OH}-\mathrm{W}_N]$ is the energy of a cluster with the hydroxyl radical and N water molecules.

The binding energy $\Delta E_{b,N}$ is given by

$$\Delta E_{b,N} = E[\mathrm{OH}-\mathrm{W}_N] - E[\mathrm{OH}] - E[W_N]. \tag{2}$$

We also define the binding enthalpy $\Delta H_{b,N}$, which is similar to the binding energy (2) but includes zero point vibrational energy corrections (ZPVE) and thermal corrections. For $N=1$, $\Delta E_{e,1} \equiv \Delta E_{b,1}$. In this case, they will be represented simply by ΔE and ΔH, respectively. Formation energies, $\Delta E_{e,N}$, calculated with the aug-cc-pVDZ basis set were corrected for basis set superposition error by using the counterpoise method[26] with fragment relaxation energy contributions.[27]

We have verified that several properties predicted by MPW1PW91/aug-cc-pVDZ calculations for the water molecule and dimer, and for the isolated hydroxyl radical are in very good agreement with experiment. These results are reported in Table I, where they are compared with experimental data for the dipole moment,[28–30] structure,[31–33] vibrational spectrum,[32,34] and energetic properties.[35,36] For OH–W_N complexes no experimental information seems to be available. Thus, we have compared the properties of the OH–W_1 complex predicted by several theoretical methods, including Møller–Pleset perturbation theory[37] at second (MP2) and fourth order (MP4), quadratic configuration interaction (QCI)[38] with the inclusion of single and double substitutions with triples and quadruples contributions to the energy [QCISD(TQ)],[39] and coupled cluster with single and double excitations (CCSD).[40–43] The results of these calculations are reported in Table I, which also includes previous theoretical data for the OH–W_1 complex from different works.[14–16] Very good agreement between DFT and *ab initio* results is observed for OH–W_1 complexes. We interpret this agreement as a strong indication on the reliability of the MPW1PW91/aug-cc-pVDZ approach to model the properties of larger OH–W_N clusters.

Monte Carlo simulations of the hydroxyl radical in water have been carried out in the isobaric–isothermal (*NPT*) ensemble[44] at $T=298$ K and $P=1$ atm. The interactions between two molecules, a and b, were described by a Lennard-Jones (LJ) plus a Coulomb contribution, with parameters ϵ_i, σ_i, and q_i for each atom:

$$U_{ab} = \sum_{i\in a}\sum_{j\in b} 4\epsilon_{ij}\left[\left(\frac{\sigma_{ij}}{r_{ij}}\right)^{12} - \left(\frac{\sigma_{ij}}{r_{ij}}\right)^{6}\right] + \frac{q_i q_j e^2}{r_{ij}}, \tag{3}$$

where $\epsilon_{ij} = (\epsilon_i \epsilon_j)^{1/2}$ and $\sigma_{ij} = (\sigma_i \sigma_j)^{1/2}$.

The SPC potential proposed by Berendsen *et al.*[45] has been adopted to represent the interactions between the water molecules. For the hydroxyl radical the Lennard-Jones parameters are the same as the SPC model for water.

To model the Coulomb interactions between the solute (hydroxyl radical) and the water molecules the charge distribution of the hydroxyl radical has been determined in the most energetically stable OH–W_5 isomer (see Fig. 2). The charge distribution of the water molecules in this cluster was represented by SPC charges and a quantum mechanical DFT calculation at the MPW1PW91/aug-cc-pVDZ level has been carried out to calculated Merz–Kollman–Singh charges[46,47] of the OH radical. This procedure takes into account, at least partially, the polarization of the OH radical by the closest water molecules. The structure of the cluster has been determined by the DFT optimizations previously described. Lennard-Jones parameters, charge distributions, and dipole moments for the OH radical and water molecule are reported in Table II.

The Monte Carlo simulations have been carried out with one solute molecule and $N=250$ water molecules. A cubic cell with periodic boundary conditions was used. The interactions were truncated at a cutoff distance R_c of 9.6 Å. The initial configuration has been generated randomly. We have carried out 10^8 steps for equilibration. Average values have been calculated over 12.5×10^8 additional steps. Each step involves the attempt to move one molecule of the system.

H_{sx} and H^*_{ss} represent, respectively, the total enthalpies of the solution (with one solute molecule) and pure liquid water, for systems with N water molecules. The total enthalpies are defined as

$$H_{sx} = E_{sx} + E_{ss} + PV \tag{4}$$

and

$$H^*_{ss} = E^*_{ss} + PV^*, \tag{5}$$

where E_{sx} is the solute–solvent energy, E^*_{ss} and E_{ss} the solvent–solvent energies in the pure liquid and solution, and V^* and V are, respectively, the volumes of the pure liquid and solution.

The hydration enthalpy of the OH radical $\Delta_{\mathrm{hyd}}H(\mathrm{OH,g})$, can be calculated as

$$\Delta_{\mathrm{hyd}}H(\mathrm{OH,g}) = H_{sx} - H^*_{ss} - RT \tag{6}$$

$$= E_{sx} + (E_{ss} - E^*_{ss}) + P(V - V^*) - RT \tag{7}$$

$$= E_{sx} + \Delta H_R - RT, \tag{8}$$

where

$$\Delta H_R = \Delta E_R + P\Delta V_R = H_{ss} - H^*_{ss} \tag{9}$$

is the solvent relaxation enthalpy. We note that a very large number of configurations is necessary to attain convergence of this quantity, which is calculated as the difference between two large fluctuating numbers.[48–50]

The DFT calculations were carried out with the GAUSSIAN 98 program.[51] The Monte Carlo simulations were carried out with the DICE program.[52]

Downloaded 27 May 2007 to 194.117.6.7. Redistribution subject to AIP license or copyright, see http://jcp.aip.org/jcp/copyright.jsp

TABLE I. Theoretical results for water, hydroxyl radical, water dimer, and hydroxyl–water complex. Dipole moment (μ) in D; distances in Å; angles in degrees; frequencies (ν) in cm^{-1}; binding energy (ΔE) and enthalpy (ΔH) in kJ mol^{-1}. MPW1PW91 and MP2 results are from geometry optimizations with the aug-cc-pVDZ basis set. MP4, QCISD(TQ), and CCSD results are single-point energy calculations with the same basis set in the MPW1PW91 geometry.

	H_2O		OH			
	MPW1PW91	Expt.	MPW1PW91	Expt.		
μ	1.872	1.855[a]	1.655	1.66[b]		
d(O–H)	0.961	0.957[c]	0.975	0.970[d]		
A(H–O–H)	104.6	104.5[c]				
ν_1	3968	3756[e]	3750	3738[e]		
ν_2	3855	3657[e]				
ν_3	1630	1595[e]				
	MPW1PW91	MP2(SDTQ)	MP4(SDTQ)	QCISD(TQ)	CCSD	Expt.
$(H_2O)_2$[f]						
μ	2.59	2.02	2.65			2.60[g]
ΔE	−20.1	−22.3	−22.5	−21.9	−20.8	−20.9±0.5[h]
ΔH^{373}	−15.5	−14.6				−15.1±0.5[i]
d(O–O)	2.892	2.911				2.976[j]
OH–(H_2O)DA(1)[f]						
μ	4.02	4.19	4.17			
ΔE	−23.8	−24.9	−24.8	−24.3	−23.3	
	[−24.4][k]	[−24.9][k]		[−23.6][l]		
ΔH^{298}	−18.1	−19.1				
d(O–H)	0.984	0.981				
OH–(H_2O)DA(3)						
μ	1.057	0.734	1.07			
ΔE	−14.3	−15.8	−15.9	−15.99	−14.7	
	[−14.8][k]					
ΔH^{298}	−9.7	−11.0				
d(O–H)	0.976	0.976				
OH–(H_2O)DD(2)						
μ	0.321	0.300				
ΔE	−15.5	−9.4[m]	−11.2	−12.4	−10.5	
	[−19.5][n]					
ΔH^{298}	−10.1					
d(O–H)	0.972					

[a]From Shepard *et al.* (Ref. 28).
[b]From Nelson *et al.* (Ref. 29).
[c]From Benedict *et al.* (Ref. 31).
[d]From Huber *et al.* (Ref. 32).
[e]From Shimanouchi (Ref. 34).
[f]PM3 semiempirical values for binding energies and enthalpies. $(H_2O)_2$: $\Delta E=-14.6$ kJ mol^{-1}; $\Delta H^{298}=-7.3$ kJ mol^{-1}. OH–W_1DA(1): $\Delta E=-16.3$ kJ mol^{-1}; $\Delta H^{298}=-8.1$ kJ mol^{-1}.
[g]From Kuchitsu and Morino (Ref. 30).
[h]From Feyerisen *et al.* (Ref. 36).
[i]From Curtiss *et al.* (Ref. 35).
[j]From Outdola and Dyke (Ref. 33).
[k]B3LYP/6-311++G(2*d*,2*p*) from Wang *et al.* (Ref. 14).
[l]CISD with triple-ζ basis set including two sets of polarization functions (TZ2P). From Xie *et al.* (Ref. 15).
[m]Single-point energy calculation with the geometry optimized at MPW1PW91/aug-ccpVDZ.
[n]B3LYP/6-311++G(2*d*,2*p*) from Zhou *et al.* (Ref. 16).

III. MICROSOLVATION MODELING

A. Energetic properties

The structure of OH–W_N clusters should reflect the ability of the OH radical to form hydrogen bonds at both ends. Thus, energetic properties of OH–W_N clusters will also be related to the energy differences between structures where the radical plays the role of a proton–acceptor and/or a proton–donor species. We will name these structures as donor–acceptor (DA). In addition, there is some indication from the present DFT calculations that other isomers are possible, where both hydrogen atoms of the water molecule interact with the OH radical oxygen and the OH hydrogen

TABLE II. Lennard-Jones (LJ) parameters, charge distribution, and dipole moment for the hydroxyl radical and water.

OH,H_2O	ϵ (kJ mol^{-1})	σ (Å)
O	0.648	3.165
H	0	0
q (a.u.)	OH	H_2O
O	−0.476	−0.820
H	0.476	0.410
μ (D)	2.3[a]	2.27[b]

[a]Calculated at the MPW1PW91/aug-cc-pVDZ level in the OH–W_5(1) conformer. The charges of the water molecules were represented by SPC charges.
[b]SPC water dipole moment.

Downloaded 27 May 2007 to 194.117.6.7. Redistribution subject to AIP license or copyright, see http://jcp.aip.org/jcp/copyright.jsp

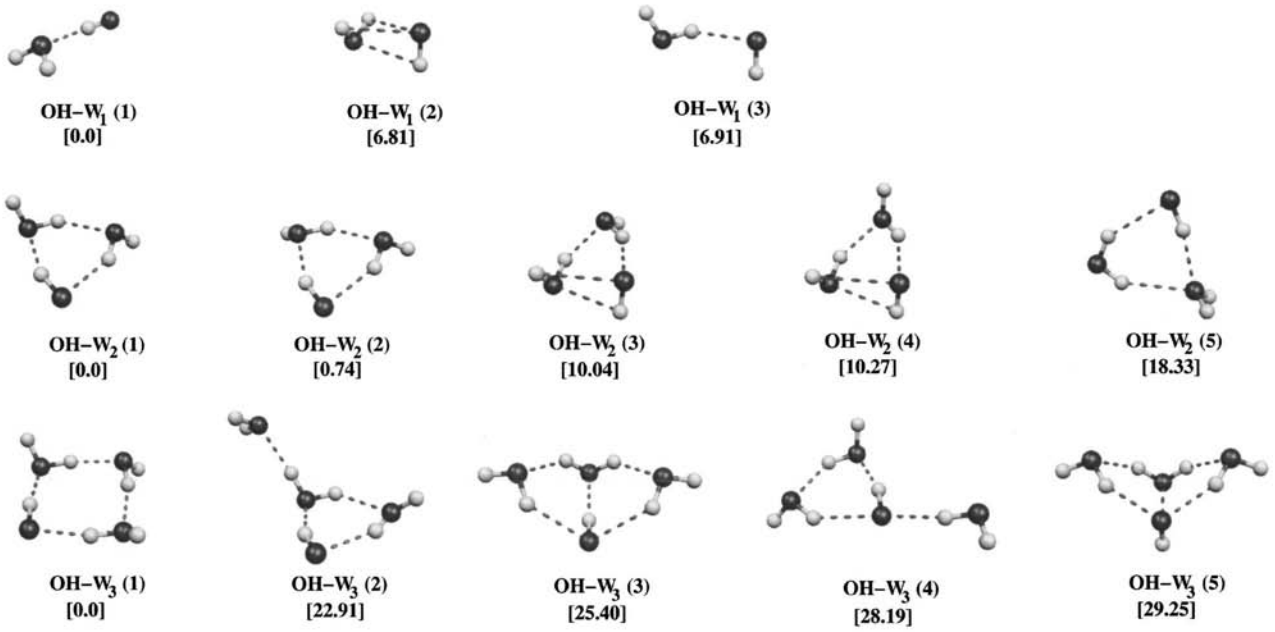

FIG. 1. Structure of the optimized OH–W_N clusters ($N=1-3$). The first structure (1) is the most stable isomer. Energy differences (including ZPVE) in kJ mol^{-1} relative to the isomer (1) are shown in brackets.

forms a weak hydrogen bond with the water oxygen [see the OH–W_1 (2) isomer in Fig. 1]. This class of isomers will be called dipole–dipole structures (DD), since they are clearly stabilized by OH radical–water antiparallel dipolar interactions. The present OH–W_1 DD complex is similar to a local minimum structure from DFT calculations, reported by Zhou *et al.*[16]

The optimized structures of the different OH–W_N isomers are shown in Fig. 1 ($N=1-3$) and Fig. 2 ($N=4-6$). These structures are local minima on the potential energy surface. Energy differences (in kJ mol^{-1}) relative to the most stable isomer (1) are reported in Figs. 1 and 2. They were calculated at the MPW1PW91/aug-cc-pVDZ level and include ZPVE.

Energetic properties for the most stable isomers of the OH–W_N clusters ($N=1-6$) are reported in Table III. We have investigated the importance of basis set superposition error (BSSE) on the evaluation of formation energies, $\Delta E_{e,N}$'s. BSSE is less than ~1% of the uncorrected values at the MPW1PW91/aug-cc-pVDZ level. Thus, BSSE is not significant in the present calculations for the formation energies and binding enthalpies, whose final values are single-point energy calculations with the larger aug-cc-pVTZ and aug-cc-pVQZ basis sets.

Water clusters have been the subject of several theoretical investigations.[53–60] Energetic properties of W_{N+1} clusters ($N=1-6$) are also reported in Table III. The present results for $\Delta E_{e,N}$'s are in very good agreement with those reported by Lee *et al.*,[59] which were based on MP2/TZ2P++ calculations. For example, for the water cyclic hexamer, $\Delta E_{e,n} = -181.0$ kJ mol^{-1} (MPW1PW91/aug-cc-pVQZ), which is in excellent agreement with the MP2/TZ2P++ value reported by Lee *et al.* (-182.1 kJ mol^{-1}).[59] For the heptamer (prism conformer) our $\Delta E_{e,n} = -219.4$ kJ mol^{-1}, which is very close to the value reported by Kim *et al.*[58] (-215.8 kJ mol^{-1}) from MP2/TZ2P++ calculations including full BSSE corrections.

It is interesting to compare binding enthalpies of the OH–W_1 complex and the water dimer. The MPW1PW91/aug-cc-pVQZ result for the water dimerization enthalpy is -12.3 kJ mol^{-1}, which is in very good agreement with the experimental result (-15.0 ± 2 kJ mol^{-1}).[35] For the OH–W_1 complex we predict that the binding enthalpy is -17.3 kJ mol^{-1} (MPW1PW91/aug-cc-pVQZ), which is ~5 kJ mol^{-1} more negative than the water dimerization enthalpy, illustrating the stability of the OH–W_1 complex, where the OH radical plays the role of proton donor. The present value is in excellent agreement with the prediction by Wang *et al.* (-16.9 kJ mol^{-1})[14] based on a Becke3LYP/6-311++G($2d,dp$) calculation for the OH–W_1 binding enthalpy. No experimental value seems to be available for comparison.

A relevant feature characterizing OH–W_N and W_{N+1} clusters is hydrogen bonding co-operativity, i.e., binding energies are strongly dependent on the cluster size, due to the nonadditive polarization effects induced by hydrogen bonding. This is illustrated in Fig. 3, where the binding enthalpy $\Delta H_{b,N}$ of OH–W_N and W_{N+1} are compared. Our results, based on MPW1PW91/aug-cc-pVQZ calculations, show that in OH–W_N clusters, $-\Delta H_{b,N}$ increases from 17.3 kJ mol^{-1} ($N=1$) to 41.3 kJ mol^{-1} ($N=3$), and then decreases to 28.2 kJ mol^{-1} ($N=6$).

In W_{N+1} clusters, $-\Delta H_{b,N}$ increases from 12.3 kJ mol^{-1} ($N+1=2$) to 42.1 kJ mol^{-1} ($N+1=4$) and then decreases to 28.5 kJ mol^{-1} ($N+1=7$). We note the remarkable stability of the water tetramer (W_4) and the OH–W_3 complex relative to other clusters. Moreover, $\Delta H_{b,N}$ for these clusters is very similar (~-41 kJ mol^{-1}). For larger clusters, the difference between $\Delta H_{b,N}$ of OH–W_N and

Downloaded 27 May 2007 to 194.117.6.7. Redistribution subject to AIP license or copyright, see http://jcp.aip.org/jcp/copyright.jsp

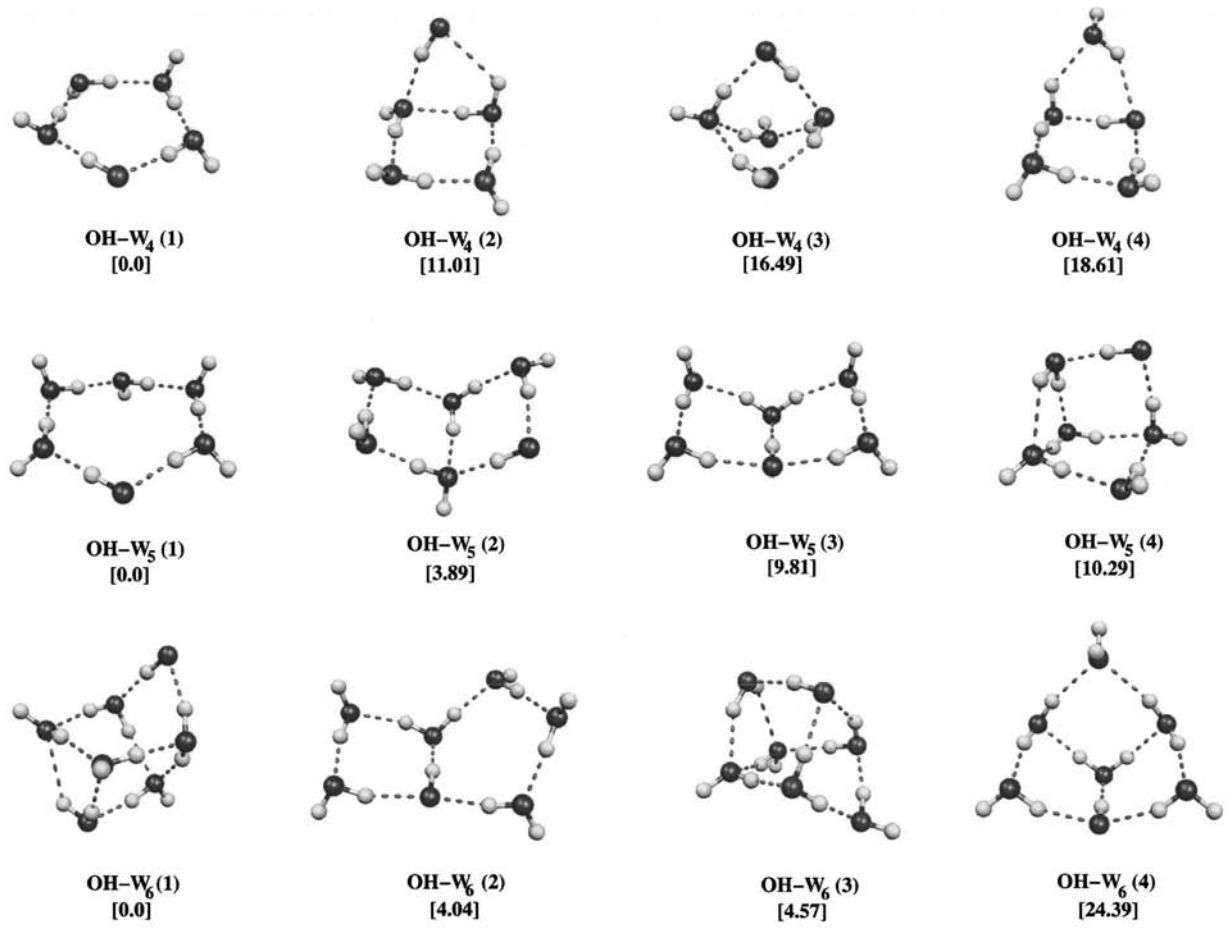

FIG. 2. Structure of the optimized OH–W_N clusters ($N=4-6$). The first structure (1) is the most stable isomer. Energy differences (including ZPVE) in kJ mol^{-1} relative to the isomer (1) are shown in brackets.

W_{N+1} clusters becomes very small. For example, when $N=4$, it is only -1.6 kJ mol^{-1}.

The behavior of $\Delta H_{b,N}$ for $N=5,6$ may suggest a convergence to some limit value close to ~ -30 kJ mol^{-1}, although extrapolations to bulk values from small clusters should be carried out with caution. For instance, the experimental water hydration enthalpy, $\Delta_{\mathrm{hyd}}H(H_2O,g) = -44.0$ kJ mol^{-1},[61] is very close to $\Delta H_{b,N} = -42.1$ kJ mol^{-1} for the W_4 cluster. However, there is a clear dependence of $\Delta H_{b,N}$ on the cluster size. For W_6, $\Delta H_{b,N} = -28.5$ kJ mol^{-1}, which is 16 kJ mol^{-1} above the experimental $\Delta_{\mathrm{hyd}}H(H_2O,g)$.

Binding energies for OH–W_N DD clusters are also reported in Table III. The binding energy of the OH–W_1 complex, -8.4 kJ mol^{-1} (aug-cc-pVQZ), is ~ 9 kJ mol^{-1} above the corresponding DA complex. Higher stability of DA clusters seems to be a general trend when we compare DA and DD isomers. This can be related to the stability of the proton–donor OH–W_1 complex, which is a building unit of all OH–W_N DA clusters.

Very recently, Hamad *et al.*[17] carried out theoretical calculations for OH–W_N clusters ($N=1-4$). They estimate that $\Delta H_{b,N}$ can be extrapolated to -20 or -25 kJ mol^{-1} from gas phase clusters and to -12 or -17 kJ mol^{-1} from a hybrid solvation model.[17] The first values (-20 or -25 kJ mol^{-1}) are in reasonable agreement with our results for OH–W_N ($N=4-6$), which range from -31.1 kJ mol^{-1} ($N=4$) to -28.2 kJ mol^{-1} ($N=6$). The extrapolations from their hybrid solvation model (-12 or -17 kJ mol^{-1}) seem to underestimate $\Delta H_{b,N}$. To discuss the electronic properties of liquid water, Coe *et al.*[12] carried out semiempirical PM3 calculations and evaluated $\Delta E_{b,N}$ for OH–W_N clusters ($N=1-15$). The extrapolated value of this quantity, based on a fitting procedure for water droplets is -35.7 kJ mol^{-1}. For water clusters, the same procedure leads to -37.6 kJ mol^{-1}.[12] The difference between the two quantities is only -1.9 kJ mol^{-1}, in good agreement with our prediction that in small clusters, $\Delta H_{b,N}$ for OH–W_N and W_{N+1} are similar.

B. Structural and vibrational properties

Structural and vibrational properties of the OH–W_N and W_{N+1} clusters are reported in Table IV. In agreement with results for energetic properties, important geometric dependence on the cluster sizes is observed. The most important changes concern the intramolecular O–H distance in the hydroxyl radical, d(O–H), which increases from 0.975 Å in the isolated radical to 1.007 Å in the OH–W_5 DA cluster. The structural changes related to the role played by the hydroxyl radical as hydrogen acceptor, d(HO...HOH), and hy-

Downloaded 27 May 2007 to 194.117.6.7. Redistribution subject to AIP license or copyright, see http://jcp.aip.org/jcp/copyright.jsp

TABLE III. Formation and binding energies (kJ mol^{-1}) for the most stable clusters of the hydroxyl radical with N water molecules (OH–W$_N$) and for water clusters (W$_{N+1}$).

DA[a]	OH–W$_1$	OH–W$_2$	OH–W$_3$	OH–W$_4$	OH–W$_5$	OH–W$_6$
			aug-cc-pVDZ			
$\Delta E_{e,N}$	−23.8	−62.0	−111.7	−151.8	−186.5	−229.8
$\Delta H_{b,N}$	−18.1	−35.7	−43.2	−32.7	−29.6	−33.3
			aug-cc-pVTZ[b]			
$\Delta E_{e,N}$	−23.1	−59.7	−108.1	−147.1	−180.7	−219.8
$\Delta H_{b,N}$	−17.4	−34.1	−41.8	−31.5	−28.3	−29.1
			aug-cc-pVQZ[b]			
$\Delta E_{e,N}$	−23.0	−59.1	−107.1	−145.6	−178.9	−217.2
$\Delta H_{b,N}$	−17.3	−33.7	−41.3	−31.1	−28.0	−28.2
			aug-cc-pVDZ(BSSE)			
$\Delta E_{e,N}$	−22.6	−58.8	−106.6	−145.0	−178.1	−216.2
E(BSSE)	1.2	3.2	5.1	6.7	8.4	13.6
DD[c]	OH–W$_1$	OH–W$_2$	OH–W$_3$			
			aug-cc-pVDZ			
$\Delta E_{e,N}$	−15.5	−51.7	−83.0			
$\Delta H_{b,N}$	−10.1	−24.9	−13.0			
			aug-cc-pVTZ[b]			
$\Delta E_{e,N}$	−14.0	−48.3	−77.3			
$\Delta H_{b,N}$	−8.7	−24.7	−9.5			
			aug-cc-pVQZ[b]			
$\Delta E_{e,N}$	−13.7	−47.6	−76.3			
$\Delta H_{b,N}$	−8.4	−24.2	−9.0			
Water clusters	W$_2$	W$_3$	W$_4$	W$_5$	W$_6$	W$_7$
			aug-cc-pVQZ[b]			
$\Delta E_{e,N}$[d]	−19.2	−60.4	−110.0	−146.1	−181.0	−219.4
	(−20.4)	(−63.3)	(−111.9)	(−147.3)	(−182.1)	(−231.4)
						[−215.8]
$\Delta H_{b,N}$	−12.3	−33.1	−42.1	−29.5	−28.2	−28.5

[a]Donor–acceptor OH–W$_N$ structures.
[b]Single-point energy calculation. Geometry optimized at MPW1PW91/aug-cc-pVDZ.
[c]Dipole–dipole OH–W$_N$ structures.
[d]Values in parentheses are MP2/TZ2P++ calculations with half BSSE correction from Lee *et al.* (Ref. 59). Bracketed value for the prism heptamer conformer (MP2/TZ2P++ calculation with full BSSE correction) is from Kim *et al.* (Ref. 58).

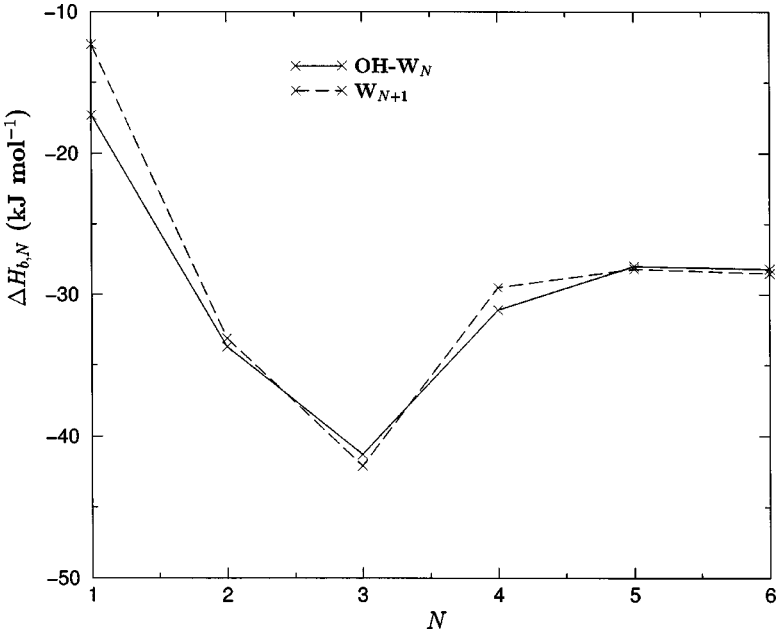

FIG. 3. Binding enthalpy ($\Delta H_{b,N}$ in kJ mol^{-1}) for OH–W$_N$ clusters and for W$_{N+1}$ clusters as a function of N, the number of water molecules (W) in the cluster.

Downloaded 27 May 2007 to 194.117.6.7. Redistribution subject to AIP license or copyright, see http://jcp.aip.org/jcp/copyright.jsp

TABLE IV. Structural and vibrational data for hydroxyl–water ($OH–W_N$) and water (W_{N+1}) clusters. Frequencies in cm^{-1}; distances in Å. Results are from MPW1PW91/aug-cc-pVDZ optimizations.

DA[a]	OH	$OH–W_1$ (1)	$OH–W_2$ (1)	$OH–W_3$ (1)	$OH–W_4$ (1)	$OH–W_5$ (1)
ν(O–H)	3750 [3738][b] [3554.1][c]	3562 [3452.2]±0.5[d] [3453.5][e]	3382	3188	3124	3105
d(O–H)[O–H]	0.975	0.984	0.994	1.003	1.006	1.007
d(HO...HOH)			1.996	1.820	1.780	1.762
d(OH...OH_2)		1.870	1.798	1.681	1.643	1.629
d(O–O)		2.854	2.784	2.717	2.693	2.682
(DD)[f]	OH	$OH–W_1$ (2)	$OH–W_2$ (3)	$OH–W_3$ (3)		
ν(O–H)	3750	3782	3795	3820		
d(O–H)[O–H]	0.975	0.972	0.971	0.969		
d(HO...HOH)		2.425	1.915	1.945		
d(OH...OH_2)		2.444	2.293	2.289		
d(O–O)		2.467	2.643	2.785		
	W_1	W_2	W_3	W_4	W_5	W_6
ν(O–H)	3968	3791	3616	3441	3377	3355
d(O–H)	0.961	0.969	0.977	0.985	0.987	0.987
d(HOH...OH_2)		1.929	1.873	1.738	1.706	1.693
d(O–O)		2.892	2.770	2.709	2.691	2.679

[a]Donor–acceptor $OH–W_N$ structures.
[b]Gas phase value from Huber *et al.* (Ref. 32).
[c]OH in argon matrix (Ref. 65).
[d]$OH–W_1$ in argon matrix (Ref. 64).
[e]$OH–W_1$ in argon matrix (Ref. 62).
[f]Dipole–dipole $OH–W_N$ structures. The most stable DD isomer has been selected.

drogen donor, d(OH...OH_2), are very similar and these distances are reduced by ~0.24 Å from $OH–W_1$ to $OH–W_5$. The average O–O distance, d(O–O), changes from 2.854 Å in $OH–W_1$ to 2.682 Å in $OH–W_5$. The same effect is observed in the water clusters where d(O–O) is reduced by 0.21 Å from W_2 to W_6.

The structure of $OH–W_N$ DD clusters shows a very interesting and specific dependency on the cluster size. Although d(O–H) is almost constant when we compare the $OH–W_1$ (0.975 Å) and $OH–W_3$ (0.969 Å) clusters, d(HO...HOH) is reduced by 0.48 Å. In contrast with W_{N+1} and $OH–W_N$ DA structures, the average distance between oxygen atoms in DD structures, d(O–O), increases by 0.32 Å from $OH–W_1$ to $OH–W_3$ clusters.

The present results for $OH–W_N$ and W_{N+1} clusters indicate a strong redshift, $\Delta\nu$, relative to isolated species (OH radical and water molecule) of the vibrational mode associated with the intramolecular O–H stretch frequency. Thus, ν(O–H) changes from 3750 cm^{-1} in the isolated radical to 3105 cm^{-1} in $OH–W_5$. A significant redshift is also observed in water clusters where ν(O–H) changes from 3968 cm^{-1} in the water monomer to 3355 cm^{-1} in W_6.

Frequency shifts ($\Delta\nu$) for the most stable $OH–W_N$ and W_{N+1} isomers as a function of N are shown in Fig. 4. Our results indicate that $\Delta\nu$ is larger in $OH–W_N$ clusters than in water clusters, mainly when $N \geqslant 3$. Experimental results for $OH–W_N$ clusters are relatively scarce although some works on the $OH–W_1$ complex in rare gas matrices have been reported.[62–66] A recent spectroscopic investigation based on the generation of the OH–W complexes in argon matrices[62] suggested that $\nu(O–H) = 3453.5\ cm^{-1}$ should be assigned to the $OH–W_1$ complex. This value is 100 cm^{-1} lower than ν(O–H) for the radical in the matrix (3554.1 cm^{-1}).[65] For $OH–W_1$, we predict that $\Delta\nu = 188\ cm^{-1}$, which is significantly higher than the experimental shift in argon matrix. However, comparison between harmonic gas phase frequencies and data in rare gas matrices is not direct. There is experimental[66] and theoretical[67] evidence that the interactions of the guest species with the matrix atoms may strongly influence the vibrational spectrum.

IV. MONTE CARLO SIMULATIONS

A. Energetics of the OH radical hydration

Thermodynamic properties for the hydrated hydroxyl radical and for pure water, obtained from *NPT* Monte Carlo simulations are reported in Table V. We first note that the densities of the solution of the hydroxyl radical in water and pure liquid water are identical (1.1 $g\,cm^{-3}$). In addition, the solvent relaxation energy induced by the hydration of the OH radical and by the water molecule differ by 7.1 $kJ\,mol^{-1}$. ΔH_R for the hydroxyl radical and water are 38.7±3.9 and 45.8±3.9 $kJ\,mol^{-1}$, respectively.

From Monte Carlo (MC) simulations, the hydration enthalpy of the OH radical, $\Delta_{hyd}H$(OH,g), is −39.1 ±3.9 $kJ\,mol^{-1}$. No experimental result is available for comparison. On the other hand, the MC result for $\Delta_{hyd}H(H_2O,g)$ is −47.9±3.9 $kJ\,mol^{-1}$, in very good agreement with experiment (−44.0 $kJ\,mol^{-1}$).[61] Thus, in keeping with the results based on the microsolvation model, our MC results in-

Downloaded 27 May 2007 to 194.117.6.7. Redistribution subject to AIP license or copyright, see http://jcp.aip.org/jcp/copyright.jsp

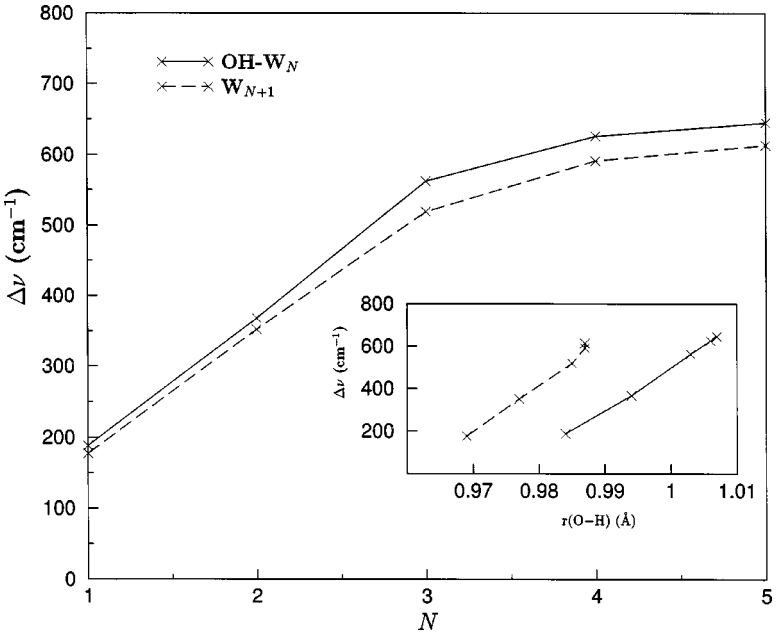

FIG. 4. O–H frequency shift $\Delta\nu$ (in cm^{-1}) vs the number of water molecules (N) in OH–W$_N$ and W$_{N+1}$ clusters ($N=1-5$). The inset shows $\Delta\nu$ vs the O–H bond length (in Å).

dicate that the hydration enthalpy of the OH radical is not very different from the hydration enthalpy of water.

We predict that the hydration energy of the hydroxyl radical, $\Delta_{\text{hyd}}E(\text{OH,g})$ is -36.6 kJ mol^{-1}. Although this result is very close to the extrapolated value of Coe *et al.* (-35.7 kJ mol^{-1}),[12] the agreement may be fortuitous. In fact, their extrapolation was based on PM3 calculations and the energetic properties of OH–W$_1$ and W$_2$ predicted by this method are not in good agreement with experiment (see Table I). Not surprisingly, however, our $\Delta_{\text{hyd}}E(\text{OH,g})$ leads to a value for the band gap of liquid water (6.88 eV) in excellent agreement with the result reported by Coe *et al.* (6.9 eV).[12] The present estimate has assumed that the vacuum level V_0 (minus the energy to promote a delocalized conducting electron of minimal energy into vacuum with zero kinetic energy) is -0.12 eV (see Coe *et al.*[12] for details on the water band gap estimation).

TABLE V. Thermodynamic properties for the hydrated hydroxyl radical and pure water from *NPT* Monte Carlo simulations at $T=298$ K and $P=1$ atm. Energies in kJ mol^{-1}. N is the number of water molecules: R_c (Å) is the cutoff radius for the interactions; ρ and ρ^* are, respectively, the densities (g/cm^3) of pure liquid and solution; E_{sx} is the solute–solvent interaction energy; $H_{ss}=E_{ss}+PV$ is the enthalpy of the water in the solution; $H^*_{ss}=E^*_{ss}+PV^*$ is the enthalpy of pure liquid water, where E^*_{ss} and V^* are the energy and volume of pure liquid water; $\Delta_{\text{hyd}}H(\text{OH,g})$ and $\Delta_{\text{hyd}}H(\text{H}_2\text{O,g})$ are the hydration enthalpies of the hydroxyl radical and water, respectively.

N	250
R_c	9.6
Hydroxyl radical in water	
ρ	1.1
E_{sx}	-75.3 ± 0.2
H_{ss}	-11304.3 ± 2.7
ΔH_R	38.7 ± 3.9
$\Delta_{\text{hyd}}H(\text{OH,g})$	-39.1 ± 3.9
Pure water (SPC model)	
ρ^*	1.1
H^*_{ss}	-11342.9 ± 2.8
ΔH_R	45.8 ± 3.9
$\Delta_{\text{hyd}}H(\text{H}_2\text{O,g})$	-47.9 ± 3.9
	$[-44.0]$[a]

[a]Experimental value from Cox *et al.* (Ref. 61).

B. Structure of the solution

The partial radial distribution functions (RDFs) for the OH radical solvated in water and pure water are shown in Figs. 5–7. Figure 5 shows the $g_{\text{O–O}}(r)$ radial distribution functions in the solution and pure liquid. The O–O RDF for the hydroxyl radical is bimodal, reflecting the hydroxyl oxygen interaction with two water molecules closer to the radical. For the hydroxyl radical this function shows two maxima (1.38 at 2.6 Å and 1.5 at 3.2 Å). Integration up to the first minimum (0.8 at 4.5 Å) yields 13.6, which is the average coordination number or the average number of water molecules in the first coordination shell of the hydroxyl radical. Although the short-range O–O correlation in pure water is quite different from the one observed for the hydrated OH radical, integration of the O–O RDF for pure water up to 4.5 Å also yields 13.6 water molecules. The average coordination numbers related to O–O correlations for the solvated O–H radical, and pure liquid water, are very close for $r \geqslant 3.7$ Å (see the inset of Fig. 5).

Figure 6 shows the $g_{\text{O–H}}(r)$ radial distribution function, which describes the correlations between the OH radical oxygen and water hydrogen atoms. These correlations are related to the role played by the OH radical as a proton acceptor in liquid water. For the hydrated OH radical this function shows a first maximum (0.6 at 1.9 Å) and integration of this function up to the first minimum (0.42 at 2.3 Å) yields 0.6, which is the average number of hydrogen atoms in close interaction with the OH oxygen atom. Comparison with the same function for liquid water shows that here the oxygen atom has a stronger interaction with the water hydro-

Downloaded 27 May 2007 to 194.117.6.7. Redistribution subject to AIP license or copyright, see http://jcp.aip.org/jcp/copyright.jsp

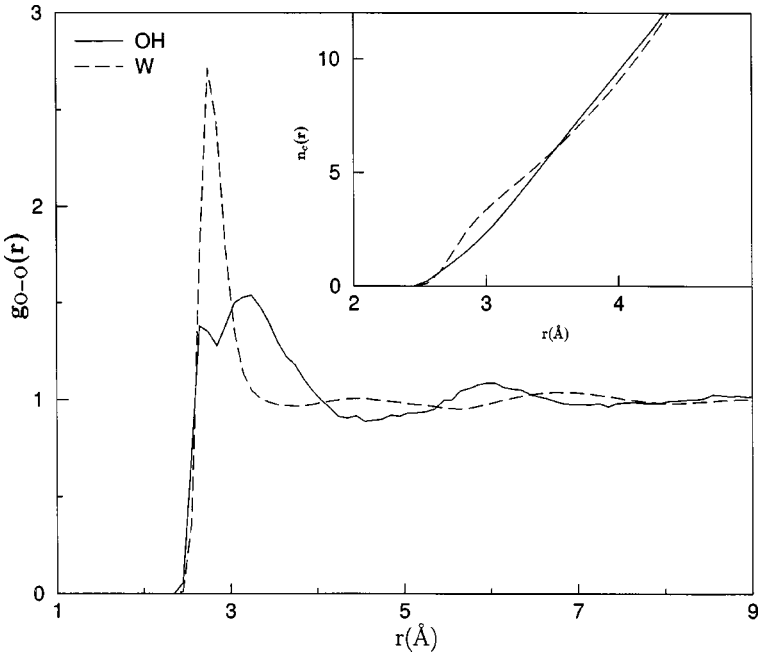

FIG. 5. Partial radial distribution function $g_{O-O}(r)$ for the hydrated OH radical and for liquid water. The inset shows the average coordination number $n_c(r)$.

gen atoms: $g_{O-H}(r)$ shows a first peak (1.3 at 1.7 Å), and integration up to the first minimum (0.25 at 2.3 Å) yields 0.94.

Figure 7 shows the $g_{H-O}(r)$ RDF, which is related to the role played by the OH radical as a proton donor in water. This function shows a sharp maximum (2.8 at 1.65 Å). Integration up to the first minimum (0.05 at 2.3 Å) yields 1.0, which is the average number of water oxygen atoms in close interaction with the OH radical hydrogen. The short-range order in the hydrated hydroxyl solution is consistent with some structural data for $OH-W_N$ clusters (Table IV). For example, $d(OH...OH_2)$ in $OH-W_1$ is 1.87 Å, which is shorter than $d(HOH...OH_2)=1.93$ Å in W_2.

Comparison between $g_{H-O}(r)$ of the hydrated OH radical and pure liquid water confirms that the short-range order is quite different for the two systems. Moreover, this function shows that the OH radical plays a more important role as a proton donor in liquid water than the water molecule. This reflects the stability of the $OH-W_1$ (1) conformer relative to the water dimer.

C. The OH dipole moment in water

Sequential Monte Carlo/DFT calculations have been carried out to analyze the polarization of the OH radical in liquid water. We have selected 50 uncorrelated supermolecular structures[18,19] with the hydroxyl radical and 2, 14, 52, 75, 100, and 125 water molecules. These numbers correspond to including all the water molecules within solvation radii of 2.85, 4.65, 7.05, 8.0, 8.8, and 9.45 Å, respectively.

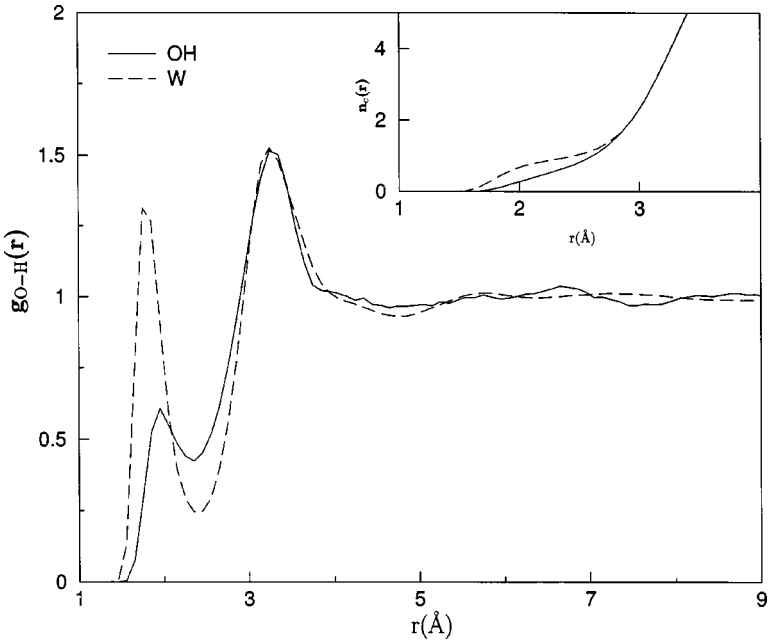

FIG. 6. Partial radial distribution function $g_{O-H}(r)$ for the hydrated OH radical and for liquid water. The inset shows the average coordination number $n_c(r)$.

Downloaded 27 May 2007 to 194.117.6.7. Redistribution subject to AIP license or copyright, see http://jcp.aip.org/jcp/copyright.jsp

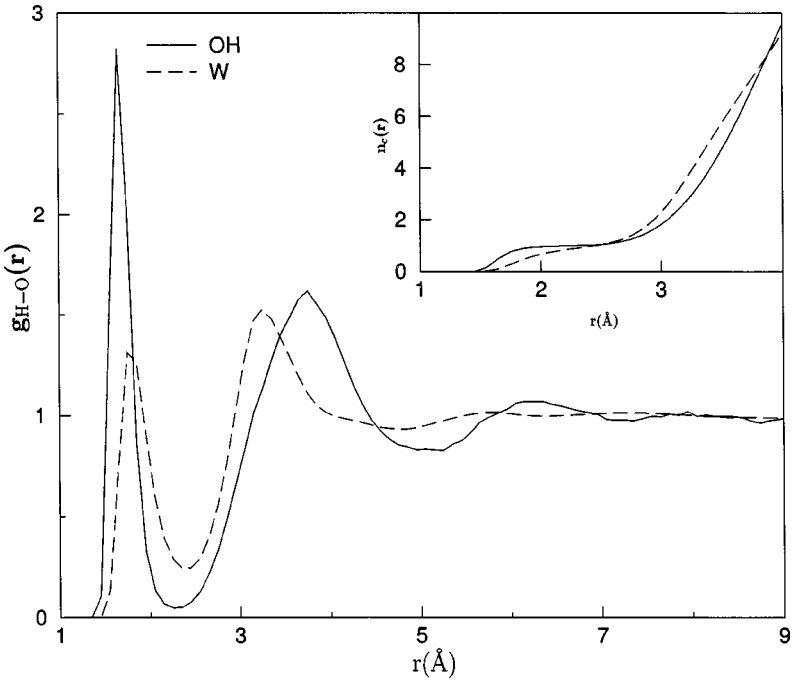

FIG. 7. Partial radial distribution function $g_{H-O}(r)$ for the hydrated OH radical and for liquid water. The inset shows the average coordination number $n_c(r)$.

Note that 14 and 52 represent the average number of water molecules in the first and second coordination shells of the hydroxyl radical. By using SPC charges on the water molecules, the average dipole moment of the solute (OH radical) over 50 uncorrelated configurations has been evaluated at the MPW1PW91/aug-cc-pVDZ level. The behavior of the induced dipole moment as a function of the number of water molecules N and the convergence of the dipole in the solution as a function of the number of uncorrelated configurations is shown in Fig. 8.

We find that the OH induced dipole moment in liquid water is $\sim 0.58 \pm 0.1$ D, which leads to an average dipole of 2.2 ± 0.1 D for the hydroxyl radical in water. This value is consistent with our parametrization of the OH radical charge distribution in the $OH-W_5$ cluster that leads to a dipole moment of 2.3 D (see Table II). It is interesting to compare the result for the OH radical with our recent prediction of the liquid water dipole moment (2.6 ± 0.14 D).[68] If we assume that the dipole moment of the water molecule in the liquid can be calculated by adding the contributions of two polarized OH dipoles of 2.2 D in the experimental geometry of the water molecule, the water dipole moment can be estimated as 2.8 D, which is only 0.2 D above our recent prediction.[68]

V. CONCLUSIONS

This work reports results for the hydration of the OH radical, including, for the first time, a theory-based predic-

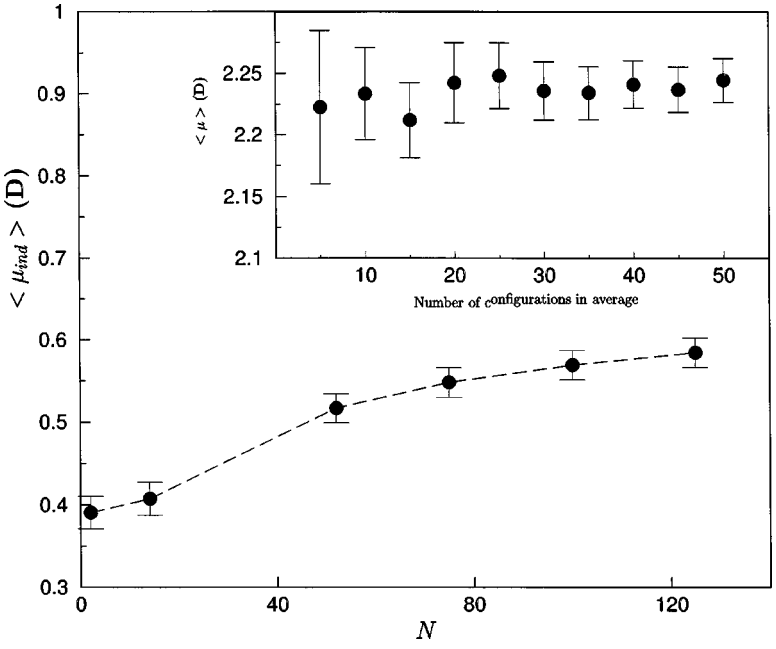

FIG. 8. Average induced dipole moment ($\langle \mu_{ind} \rangle$ in D) of the hydroxyl radical as a function of the number of water molecules N in the liquid. The inset shows the convergence of the OH average dipole moment as a function of the number of uncorrelated MC configurations.

Downloaded 27 May 2007 to 194.117.6.7. Redistribution subject to AIP license or copyright, see http://jcp.aip.org/jcp/copyright.jsp

tion for the hydration enthalpy of this species. This quantity is of fundamental interest in several domains, ranging from biochemistry to electronic properties of liquid water. The present study relies on two complementary approaches: microsolvation and statistical mechanics Monte Carlo simulations. From microsolvation modeling we conclude that for small water clusters (W_N), the binding energies of the OH radical to W_N, and of the water molecule to W_N, are very close. This can be related to the stability of the $OH–W_1$ complex, where the radical plays the role of proton donor.

Based on Monte Carlo simulations, our results show that the hydration enthalpies of the OH radical and water differ by less than 10 kJ mol^{-1}. The enthalpic stabilization of the water molecule in liquid water relative to the OH radical is possibly due to the contribution of long-ranged dipolar interactions and polarization effects. In this sense, other interesting conclusion concerns the polarization of the OH radical in liquid water. We predict that the dipole moment of the OH radical in water (2.2 ± 0.1 D) is increased by $\sim$30% in comparison with the gas phase value (1.66 D). This prediction is based on the SPC intermolecular potential, which is a very simple model. Further investigations with other intermolecular interaction models can be useful to confirm the present predictions. However, we note that our result for the OH radical dipole moment in water is consistent with a recent evaluation of the water dipole moment in liquid water (2.6 ± 0.1 D) by sequential Monte Carlo/quantum mechanics calculations,[68] based on the TIP5P[69] intermolecular potential model.

Our results for the OH radical hydration energy leads to a value for the liquid water band gap (6.88 eV) in excellent agreement with a recent prediction by Coe *et al.*[12]

ACKNOWLEDGMENTS

R.C.G. and P.C.d.C. gratefully acknowledge the support of Fundação para a Ciência e a Tecnologia. (Ph.D. Grant Nos. PRAXIS/XXI/BD/15920/98 and PRAXIS/XXI/BD/6503/2001). This work was partially supported by the Sapiens program of the FCT, Portugal (Grant No. POCTI/43315/QUI/2001).

[1] B. Halliwell and J. H. C. Gutteridge, *Free Radicals in Biology and Medicine* (Oxford University Press, Oxford, 1989).
[2] W. H. Kopenol, Free Radical Biol. Med. **10**, 85 (1991).
[3] E. R. Stadtman, Annu. Rev. Biochem. **62**, 797 (1993).
[4] B. Aygodan, D. T. Marshall, S. G. Stwarts, J. E. Turner, A. J. Boone, N. G. Richards, and W. E. Bolch, Radiat. Res. **157**, 38 (2002).
[5] W. Linert and G. N. L. Jameson, Inorg. Chem. **79**, 319 (2000).
[6] A. K. Chandra and T. Uchimaru, J. Phys. Chem. A **104**, 8535 (2000).
[7] P.-Y. Lien, R.-M. You, and W.-P. Hu, J. Phys. Chem. A **105**, 2391 (2001).
[8] I. W. M. Smith and A. R. Ravishankara, J. Phys. Chem. A **106**, 4798 (2002).
[9] J. E. Headrick and V. Vaida, Phys. Chem. Earth. **26**, 479 (2001).
[10] T. LaVere, D. Becker, and M. D. Sevilla, Radiat. Res. **145**, 673 (1996).
[11] L. Cermenati, P. Pichat, C. Guillard, and A. Albini, J. Phys. Chem. B **101**, 2650 (1997).
[12] J. V. Coe, A. D. Earhart, M. C. Cohen, G. J. Hoffman, H. W. Sarkas, and K. H. Bowen, J. Chem. Phys. **107**, 6023 (1997).
[13] K. S. Kim, H. S. Kim, J. H. Jang, H. S. Kim, and B.-J. Mhin, J. Chem. Phys. **94**, 2057 (1991).
[14] B. Wang, H. Hou, and Y. Gu, Chem. Phys. Lett. **303**, 96 (1999).
[15] Y. Xie and H. F. Schaefer III, J. Chem. Phys. **98**, 8829 (1993).
[16] Z. Zhou, Y. Qu, A. Fu, B. Du, F. He, and H. Gao, Int. J. Quantum Chem. **89**, 550 (2002).
[17] S. Hamad, S. Lago, and J. A. Mejías, J. Phys. Chem. A **106**, 9104 (2002).
[18] S. Canuto and K. Coutinho, Adv. Chem. Phys. **28**, 90 (1997).
[19] K. Coutinho and S. Canuto, J. Chem. Phys. **113**, 9132 (2000).
[20] C. Adamo and V. Barone, Chem. Phys. Lett. **274**, 242 (1997).
[21] C. Adamo and V. Barone, J. Comput. Chem. **19**, 419 (1998).
[22] C. Adamo and V. Barone, J. Chem. Phys. **108**, 664 (1998).
[23] J. P. Perdew and Y. Wang, Phys. Rev. B **45**, 13244 (1992).
[24] D. E. Woon and T. H. Dunning, Jr., J. Chem. Phys. **98**, 1358 (1993).
[25] R. A. Kendall, T. H. Dunning, Jr., and R. J. Harrisson, J. Chem. Phys. **96**, 6796 (1992).
[26] S. F. Boys and F. Bernardi, Mol. Phys. **19**, 553 (1970).
[27] S. S. Xantheas, J. Chem. Phys. **104**, 8821 (1986).
[28] A. C. Shepard, Y. Beers, G. P. Klein, and L. S. Rothman, J. Chem. Phys. **59**, 2254 (1973).
[29] R. D. Nelson, Jr., D. R. Lide, and A. A. Maryott, *Selected Values of Electric Dipole Moments for the Molecules in the Gas Phase* (NSRDS-NBS10, Washington, DC, 1967).
[30] K. Kuchitsu and Y. Morino, Bull. Chem. Soc. Jpn. **38**, 805 (1965).
[31] W. S. Benedict, N. Gailar, and E. K. Plyler, J. Chem. Phys. **24**, 9639 (1956).
[32] K. P. Huber and G. Herzberg, *Molecular Spectra and Molecular Structure. IV. Constants of Diatomic Molecules* (Van Nostrand Reinhold, New York, 1979).
[33] A. Outdola and T. R. Dyke, J. Chem. Phys. **72**, 5062 (1980).
[34] T. Shimanouchi, *Tables of Molecular Vibrational Frequencies* (NSRDS NBS-39, Washington, DC, 1972), Consolidated Vol. 1.
[35] L. A. Curtiss, D. J. Frurip, and M. Blander, J. Chem. Phys. **71**, 2703 (1979).
[36] M. M. Feyerisen, D. Feller, and D. A. Dixon, J. Phys. Chem. **100**, 2993 (1996).
[37] C. Møller and M. S. Pleset, Phys. Rev. **46**, 618 (1934).
[38] J. A. Pople, M. Head-Gordon, and K. Raghavachari, J. Chem. Phys. **87**, 5968 (1987).
[39] K. Raghavachari, J. A. Pople, E. S. Replogle, and M. Head-Gordon, J. Phys. Chem. **94**, 5579 (1990).
[40] J. Cizek, Adv. Chem. Phys. **14**, 35 (1969).
[41] G. D. Purvis and R. J. Bartlett, J. Chem. Phys. **76**, 1910 (1982).
[42] G. E. Scuseria, C. L. Janssen, and H. F. Schafer III, J. Chem. Phys. **72**, 4244 (1980).
[43] G. E. Scuseria and H. F. Schafer III, J. Chem. Phys. **90**, 3700 (1989).
[44] D. Frenkel and B. Smit, *Understanding Molecular Simulation* (Academic, San Diego, 1996).
[45] H. J. C. Berendsen, J. P. M. Postma, W. F. van Gusteren, and J. Hermans, in *Intermolecular Forces*, edited by B. Pullman (Reidel, Dordrecht, 1981), p. 331.
[46] U. C. Singh and P. A. Kollman, J. Comput. Chem. **5**, 129 (1984).
[47] B. H. Besler, K. M. Merz, Jr., and P. A. Kollman, J. Comput. Chem. **11**, 431 (1990).
[48] V. N. Levchuk, I. I. Sheykhet, and B. Ya. Simkin, Chem. Phys. Lett. **185**, 339 (1991).
[49] T. Lazaridis, J. Phys. Chem. B **104**, 4964 (2000).
[50] R. C. Guedes, K. Coutinho, B. J. Costa Cabral, and S. Canuto, J. Phys. Chem. B **107**, 4304 (2003).
[51] M. J. Frisch, G. W. Trucks, H. B. Schlegel *et al.*, GAUSSIAN 98, Gaussian Inc., Pittsburgh, PA, 1998.
[52] K. Coutinho and S. Canuto, DICE: A general Monte Carlo program for liquid simulation, University of São Paulo, Brazil, 2000.
[53] K. S. Kim, M. Dupuis, G. C. Lie, and E. Clementi, Chem. Phys. Lett. **131**, 451 (1986).
[54] K. S. Kim, B. J. Mhin, and K. S. Kim, J. Chem. Phys. **97**, 6649 (1992).
[55] J. Kim, J. Y. Lee, S. Lee, B. J. Mhin, and K. S. Kim, J. Chem. Phys. **102**, 310 (1995).
[56] M. W. Feyereisen, D. Feller, and D. A. Dixon, J. Phys. Chem. **100**, 2993 (1996).
[57] M. Schütz, S. Brdarski, P.-O. Widmark, R. Lindh, and G. Karlström, J. Chem. Phys. **107**, 4597 (1997).
[58] J. Kim, D. Majumdar, H. M. Lee, and K. S. Kim, J. Chem. Phys. **110**, 9128 (1999).
[59] H. M. Lee, S. B. Suh, J. Y. Lee, P. Tarakeshwar, and K. S. Kim, J. Chem. Phys. **112**, 9759 (2000).
[60] K. S. Kim, P. Tarakeshwar, and J. Y. Lee, Chem. Rev. (Washington, D.C.) **100**, 4145 (2000).

Downloaded 27 May 2007 to 194.117.6.7. Redistribution subject to AIP license or copyright, see http://jcp.aip.org/jcp/copyright.jsp

[61] *CODATA Key Values for Thermodynamics*, edited by J. D. Cox, D. D. Wagman, and V. A. Medvedev (Hemisphere, New York, 1989).
[62] A. Engdahl, G. Karlström, and B. Nelander, J. Chem. Phys. **118**, 7797 (2003).
[63] P. D. Cooper, H. G. Kjaergaard, V. S. Langford, A. J. McKinley, T. I. Quickenden, and D. P. Schofield, J. Am. Chem. Soc. **125**, 6048 (2003).
[64] V. S. Langford, A. J. McKinley, and T. I. Quickenden, J. Am. Chem. Soc. **122**, 12859 (2000).
[65] L. Khriachtchev, M. Pettersson, S. Touminen, and M. Räsänen, J. Chem. Phys. **107**, 7252 (1997).
[66] J. Goodman and L. E. Brus, J. Chem. Phys. **67**, 4858 (1977).
[67] J. P. Prates Ramalho, B. J. Costa Cabral, and F. M. S. Silva Fernandes, Chem. Phys. Lett. **184**, 53 (1991).
[68] K. Coutinho, R. C. Guedes, B. J. Costa Cabral, and S. Canuto, Chem. Phys. Lett. **369**, 345 (2003).
[69] M. W. Mahoney and W. L. Jorgensen, J. Chem. Phys. **112**, 8910 (2000).

Downloaded 27 May 2007 to 194.117.6.7. Redistribution subject to AIP license or copyright, see http://jcp.aip.org/jcp/copyright.jsp